

Methods

SV40 VP1 pentamers for assembly reaction

SV40 VP1 VLPs production, disassembly and reassembly reactions were performed as described.¹ For assembly reactions, 10 nM DNA origami structure was incubated with 4 μ M disassembled VP1 pentamers in 1 \times assembly buffer (125 mM NaCl, 50 mM MOPS pH 7.2) at room temperature for 24 hours.

DNA origami

DNA origami structures of the desired sizes are commercially available from tilibit nanosystems, Garching, Germany. All relevant techniques have been previously described.²

The 30 nm nearly-spherical DNA origami structure was assembled as 100 parallel dsDNA helices of varying length arranged in a square lattice, with a 5386 nt-long scaffold DNA strand based on the *phi X 174* bacteriophage and 161 shorter staple strands. Assembly was achieved through a cooperative self-assembly process in a one-pot reaction.

The 40 nm near-spherical DNA origami structure was assembled as a dimer of two unique monomer half-sphere structures, with each monomer consisting of 104 parallel dsDNA helices of varying length arranged in a square lattice. The first monomer is based on a 7249 nt-long scaffold DNA strand based on a *M13mp18* bacteriophage derivative and 211 shorter staple strands, and the second monomer is based on a 7560 nt-long scaffold DNA strand based on a *M13mp18* bacteriophage derivative and 218 shorter staple strands. The dimer structure is stabilized through sticky ends and stacking interactions. Assembly of each monomer was achieved through a cooperative self-assembly process in a one-pot reaction. Dimer assembly was achieved in a second incubation step by mixing the two assembled monomer structures.

The 35 nm near-spherical DNA origami structure was assembled as 108 parallel dsDNA helices of varying length arranged in a honeycomb-type lattice, with a 7560 nt-long scaffold DNA strand based on a *M13mp18* bacteriophage derivative and 227 shorter staple strands. Assembly was achieved through a cooperative self-assembly process in a one-pot reaction.

Negative stain TEM

3 μl of VLP samples were applied to a glow discharged grid (carbon support film on 300 mesh Cu grids, Ted Pella, Ltd.). After 10-20 sec the excess liquid was blotted off with a filter paper. The grids were incubated with 2% Uranyl acetate stain for 30 sec, blotted and allowed to dry in air. The samples were imaged on a FEI Tecnai 12 G2 TWIN TEM operated at 120 kV and the images were recorded on a 4K x 4K FEI Eagle CCD camera.

Cryo-EM Sample preparation

3 μl VLP samples were applied to holey carbon grids (Quantifoil R 1.2/1.3, Micro Tools GmbH, Germany) after 30 seconds glow discharge treatment. Grids were blotted and vitrified by rapidly plunging into liquid ethane at -182°C with a Vitrobot (FEI, Eindhoven).^{3, 4}

Data acquisition

Samples were imaged with an FEI Tecnai F30 Polara microscope (FEI, Eindhoven) operating at 300 kV. Datasets were automatically collected using SerialEM⁵ on a K2 Summit direct electron detector camera fitted behind an energy filter (Gatan Quantum GIF) operated with a 20 eV slit around the zero loss peak. Pixel size at the sample plane was 2.3 \AA . The camera was operated in counting mode at a dose rate of 10 electrons/pixel/second. Each movie was dose fractionated into 50 frames, with total electron dose of 80 $\text{e}/\text{\AA}^2$,

Single particle reconstruction

Dose-fractionated image stacks were aligned using MotionCorr^{2, 6} and their defocus values estimated by Gctf.⁷ The aligned sums were used for further processing. The rest of the processing was done in RELION3.0 beta-2.⁸ Particles were autopicked and subjected to 2D classification. The initial 3D reference was prepared from 4200 particles of manually selected 2D class averages. We performed 3D classification of all picked 2D class averages that yielded an empty capsids class and an origami-filled class. 3D refinement of the empty capsid particles, imposing icosahedral symmetry, yielded a 7.3 \AA map and further CTF refinement followed by particle polishing gave rise to a 6.8 \AA map (EMD_4648, Fig. S2 red). The origami-filled capsid 3D class was further refined to a 21 \AA map (EMD_4651, Fig. S2 green). Applying a mask around the origami particle (capsid-masked origami in which the external capsid is excluded) and including the naked origami 2D class averages followed by 3D refinement yielded a 15 \AA

map (EMD_4652, Fig. S2 orange). Similarly, applying a mask around the capsid of the origami-filled 3D class (origami-masked capsid in which the origami is excluded), imposing icosahedral symmetry, yielded an 8.5 Å map (EMD_4653, Fig. S2 blue).

Correct handedness of the empty capsid was assessed by the quality of fit to the SV40 crystal structure (PDB ID 1SVA),⁹ and by manual inspection of the fit (see Fig. S3). Measuring correlation coefficients using the UCSF Chimera protocol “Fit in Map”,¹⁰ the correlation coefficient was 0.952 (as opposed to 0.907 for the opposite inverted map).

Movie preparation

The supplemental movie, which is intended to convey the orientation of the origami honeycomb structure (yellow) with respect to the capsid’s icosahedral symmetry (green), was prepared in UCSF Chimera.

1. Mukherjee, S.; Abd-El-Latif, M.; Bronstein, M.; Ben-nun-Shaul, O.; Kler, S.; Oppenheim, A. *PloS one* **2007**, 2, (8), e765.
2. Wagenbauer, K. F.; Engelhardt, F. A. S.; Stahl, E.; Hechtel, V. K.; Stommer, P.; Seebacher, F.; Meregalli, L.; Ketterer, P.; Gerling, T.; Dietz, H. *Chembiochem* **2017**, 18, (19), 1873-1885.
3. Dubochet, J.; Adrian, M.; Chang, J. J.; Homo, J. C.; Lepault, J.; McDowell, A. W.; Schultz, P. *Quarterly reviews of biophysics* **1988**, 21, (2), 129-228.
4. Wagenknecht, T.; Frank, J.; Boublik, M.; Nurse, K.; Ofengand, J. *Journal of molecular biology* **1988**, 203, (3), 753-60.
5. Mastrorade, D. N. *J Struct Biol* **2005**, 152, (1), 36-51.
6. Li, X.; Mooney, P.; Zheng, S.; Booth, C. R.; Braunfeld, M. B.; Gubbens, S.; Agard, D. A.; Cheng, Y. *Nat Methods* **2013**, 10, (6), 584-90.
7. Zhang, K. *J Struct Biol* **2016**, 193, (1), 1-12.
8. Kimanius, D.; Forsberg, B. O.; Scheres, S. H.; Lindahl, E. *Elife* **2016**, 5.
9. Stehle, T.; Gamblin, S. J.; Yan, Y.; Harrison, S. C. *Structure (London, England : 1993)* **1996**, 4, (2), 165-82.
10. Pettersen, E. F.; Goddard, T. D.; Huang, C. C.; Couch, G. S.; Greenblatt, D. M.; Meng, E. C.; Ferrin, T. E. *J Comput Chem* **2004**, 25, (13), 1605-12.

11. Shen, P. S.; Enderlein, D.; Nelson, C. D.; Carter, W. S.; Kawano, M.; Xing, L.; Swenson, R. D.; Olson, N. H.; Baker, T. S.; Cheng, R. H.; Atwood, W. J.; Johne, R.; Belnap, D. M. *Virology* **2011**, 411, (1), 142-52.

Supporting figures.

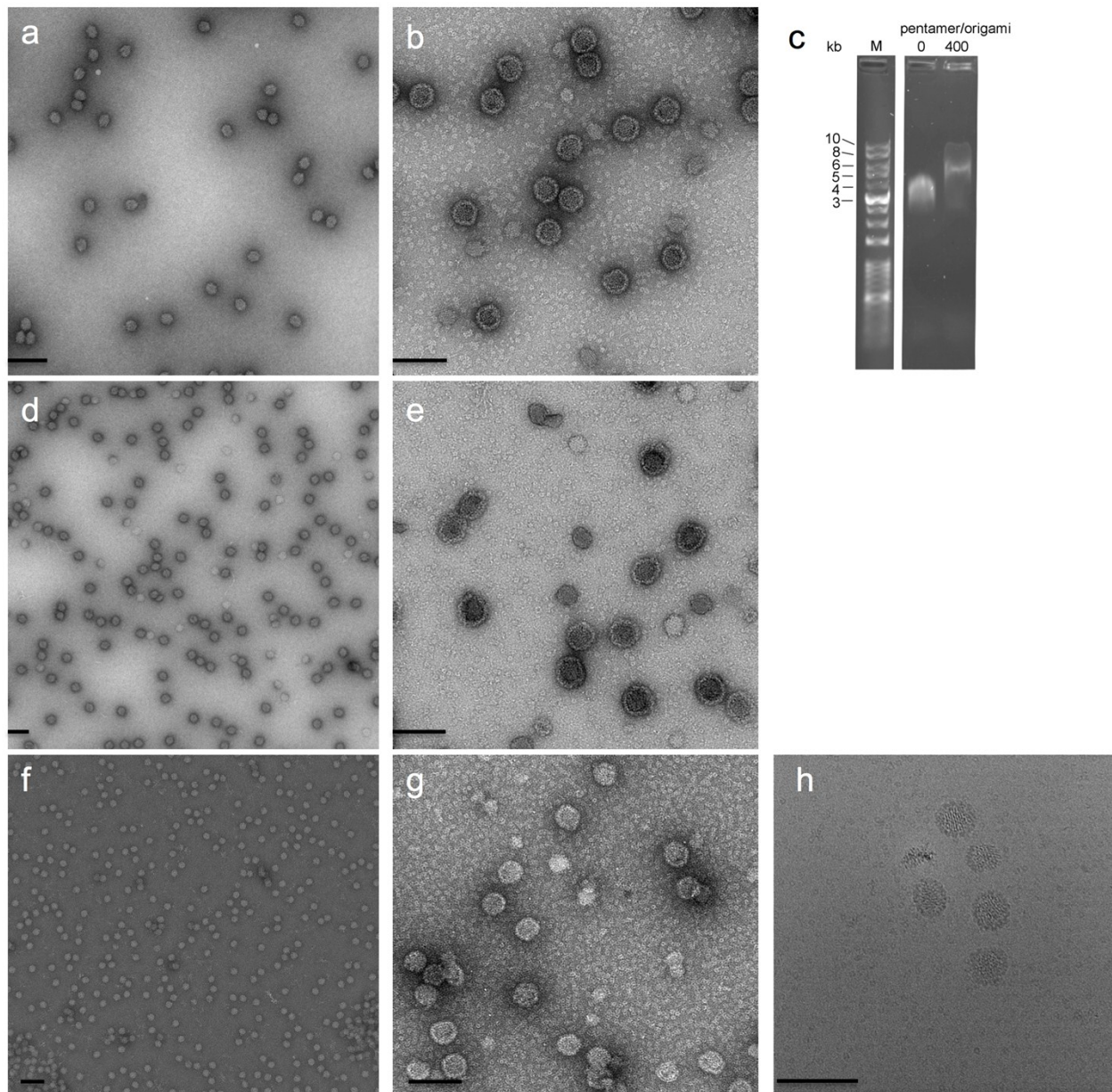


Fig. S1 VP1 assembly on DNA origami. (a) Negative stain TEM images of 35 nm DNA origami. (b) Negative stain TEM images of 50 nm particles formed on 35 nm DNA origami. (c)

Electrophoretic Mobility Shift Assay (EMSA) analysis showing formation of VP1/DNA origami complex. (d) Negative stain TEM images of 40 nm DNA origami. (e) Negative stain TEM images of particles formed on 40 nm DNA origami. (f) Negative stain TEM images of 30 nm DNA origami. (g) Negative stain TEM images of particles formed on 30 nm DNA origami. (h) Cryo-EM micrograph of particles formed on 30 nm DNA origami (scale bars, 100 nm).

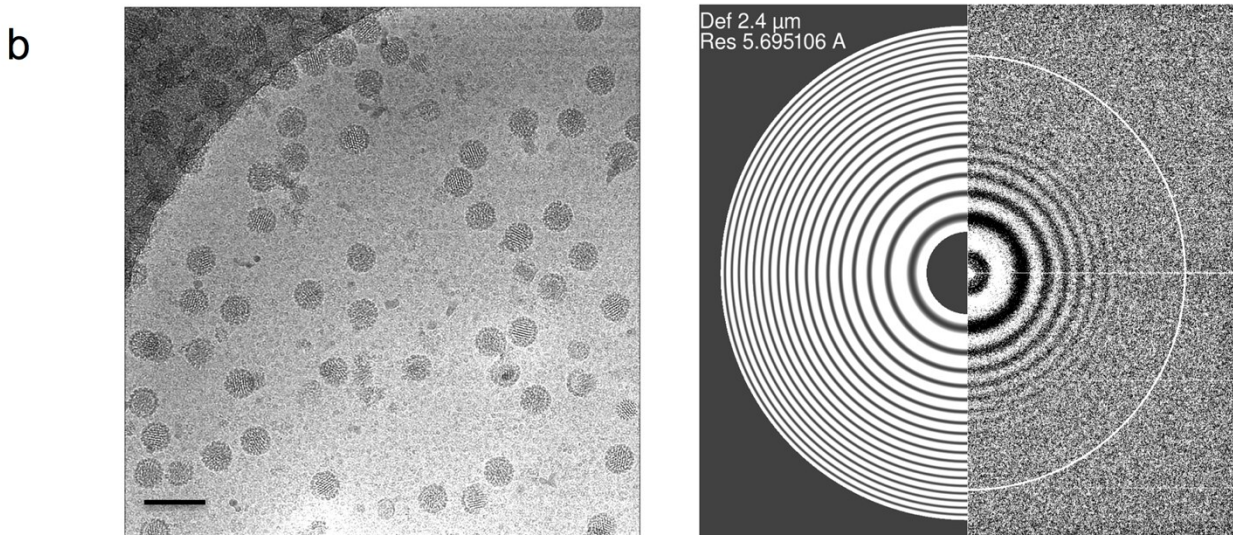
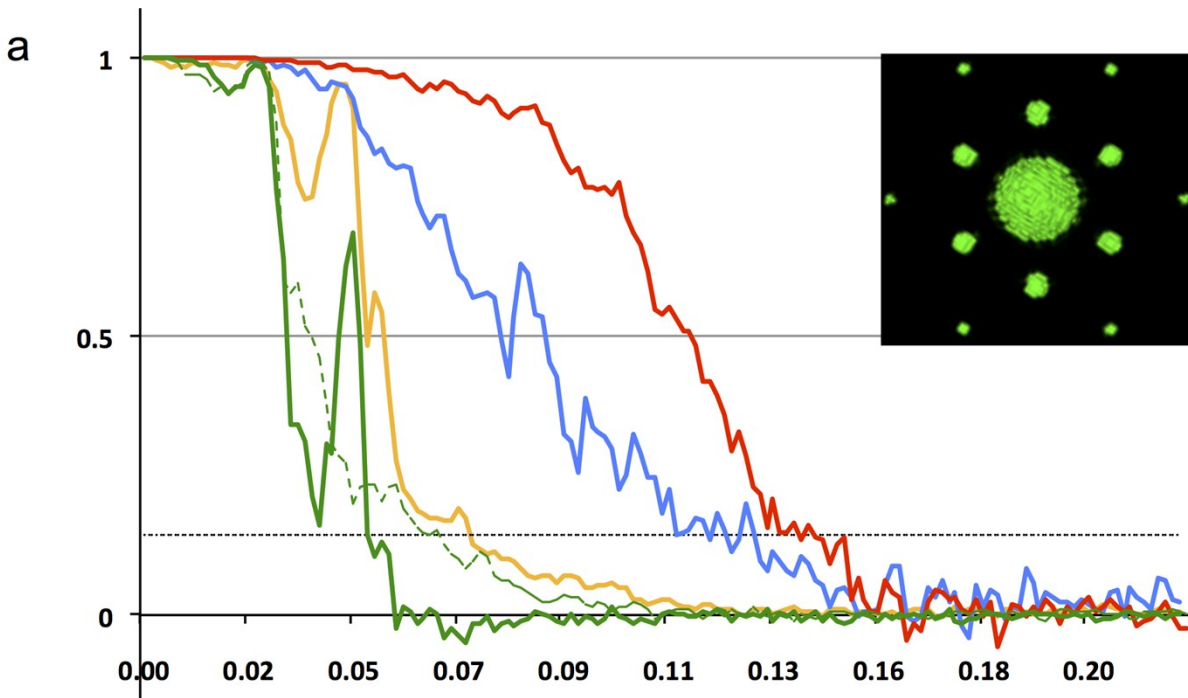


Fig. S2 Validation of image processing procedures. (a) Fourier shell correlation (FSC) plots of the different maps presented in the paper: The empty capsid map in red (presented in Fig. 1(c)). The origami filled capsid after focused refinement with a mask that excludes the internal origami (origami-masked capsid) in blue (presented in Fig. 3(a), cyan). Origami-filled capsid with no imposed symmetry in green (presented in Fig. 1(d) and 3(b)). Origami only map resulting reconstruction from a data set of non-encapsulated origami particles and externally masked origami filled capsids (capsid-masked origami) in orange (presented in Fig. 2(b)). The “gold-standard” FSC 0.143 criterion is shown as a dotted black line. The lattice structure of the DNA imposes strong modulation of the frequencies found in the electron density maps in all the 3D reconstructions that contain the origami (inset—the power spectrum of the origami-filled capsid map). As a result the FSC curves of these reconstructions have a typical dipping above the frequencies that corresponds to the length of the repeating units of the origami (~ 25 Å). In order to make sure that this is indeed the case, using a soft mask we excluded the origami from the two half maps after refinement of the origami filled capsid and recalculated the FSC curve. This procedure deleted the large dipping (dashed green). (b) A typical micrograph showing the SV40 particles and its power spectrum showing Tone rings up to 5.9 Å (scale bar is 100 nm).

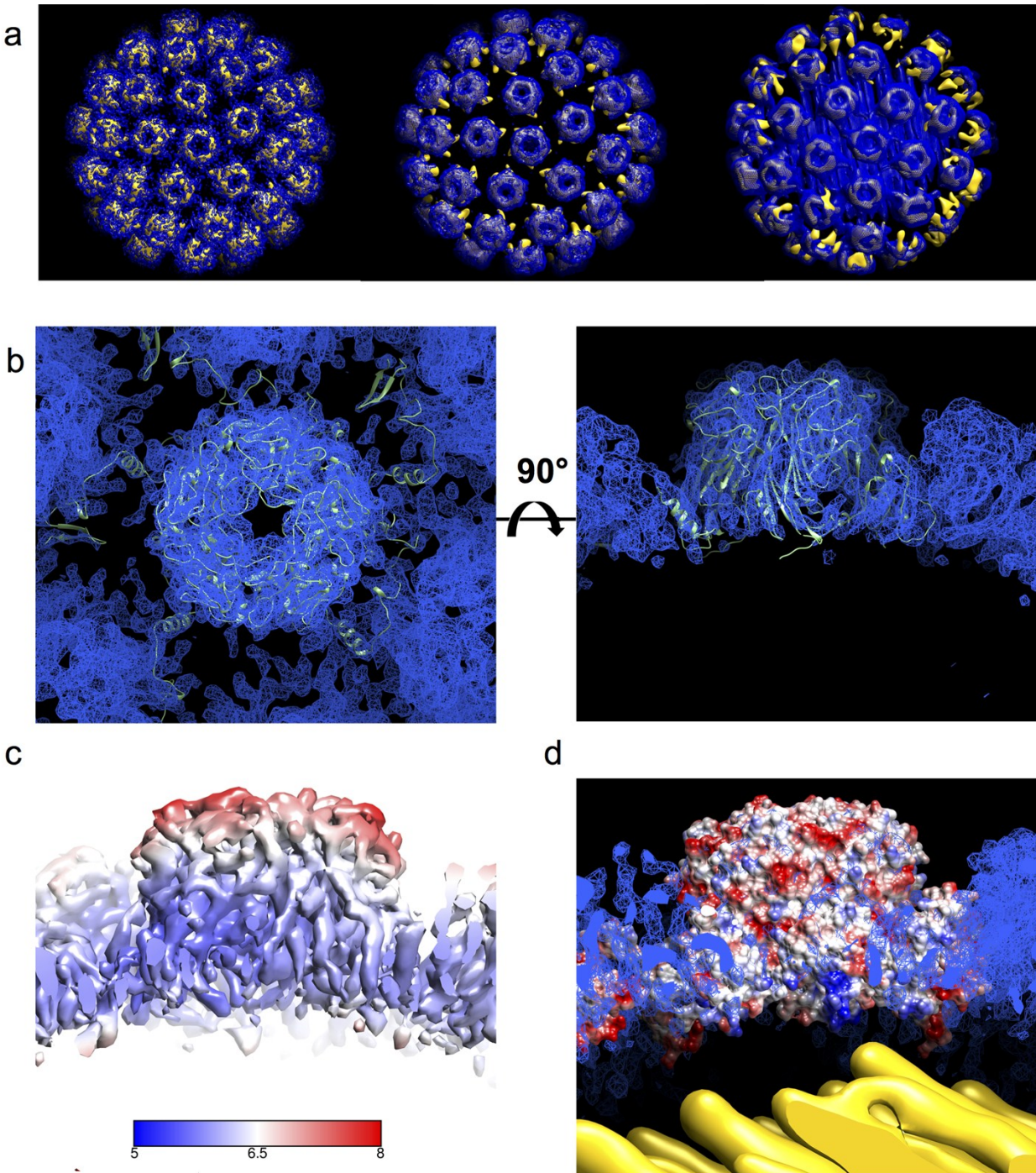


Fig. S3 (a) Fit of the density maps (in blue mesh) of the empty capsid (left), the internally masked origami filled capsids (origami-masked capsid, center) and the unmasked origami-filled (right) to the cryo-EM map of SV40 that was previously determined by Shen et al. EMD_5187¹¹ (in yellow). (b) Rigid body fit of the VP1 crystal structure to the empty capsid 6.8 Å map. Note

the density quality in the fitted atomic model displayed as ribbons. (c) Reconstruction colored by local resolution (from 5.0 Å, blue, to 8.0 Å, red) using RELION3.0, viewed from the capsid plane. (d) Electrostatic surface representation (negative in red, positive in blue) of the VP1 crystal structure shown from the plane of the capsid with the fitted masked origami map (in yellow).

Data collection				
Electron Microscope	FEI F30 Polara			
Voltage (kV)	300			
Detector	Gatan GIF Quantum K2 Summit			
Pixel size (Å)	2.3			
Electron dose (e ⁻ /Å ²)	100			
Number of frames	50			
Grid type	300 mesh Holey-carbon Quantifoil 2/2			
Number of micrographs used	980			
Defocus range (µm)	0.4-3.5			
Resolution limits (Å)	4.9-8.3			
Reconstruction				
Software	Relion 3.0 beta2			
Number of particles picked	51713			
Structure name	Empty capsid	Origami-filled	Origami-masked capsid	Capsid-masked origami (Including naked origami)
Number of particles used	13818	7939	7939	14772
Symmetry	I1	C1	I1	C1
Resolution (Å)	6.8	21	8.5	15
EMDB_ID	4648	4651	4653	4652

Table S1. Cryo-EM data collection, reconstruction parameters.